 CMES, vol.71, no.4, pp.347-362, 2011

Computation of Nonlinear Schrödinger Equation on an Open Waveguide Terminated by a PML

Jianxin Zhu [1], **Zheqi Shen**[1]

Abstract: It is known that the perfectly matched layer (PML) is a powerful tool to truncate the unbounded domain. Recently, the PML technique has been introduced in the computation of nonlinear Schrödinger equations (NSE), in which the nonlinearity is separated by some efficient time-splitting methods. A major task in the study of PML is that the original equation is modified by a factor c which varies fast inside the layer. And a large number of grid points are needed to capture the profile of c in the discretization. In this paper, the possibility is discussed for using some nonuniform finite difference schemes in spatial discretization. It is proved that the uniform refinement inside the PML will cause spurious reflections at the interface, and therefore is invalid. As a remedy, a new method for the discretization is proposed by applying an additional coordinate transformation. This method effectively reduces the error caused by the discretization of PML, and it is quite useful in long time computation of time-dependent problems in open waveguides. These discussions are essential for the further research of the numerical solutions of NSE on unbounded domains.

Keywords: nonlinear Schrödinger equation, open waveguide, PML, nonuniform discretization.

1 Introduction

The Schrödinger equation is the central equation to quantum mechanics as Newton's laws are to classical mechanics. In many cases, analytic solutions to the time-dependent Schrödinger equation (TDSE) are not obtainable, therefore numerical simulations are needed in order to obtain approximate solutions. In numerical simulations, the greatest difficulty arises from the fact that the scale of quantum mechanics is too small, which leads the equation to be defined on an almost infinite spatial domain. Under this circumstance, the domain should be restricted into a

[1] Department of Mathematics, Zhejiang University, Hangzhou 310027, China, e-mail: zjx@zju.edu.cn

small scale by doing some truncations, such as some artificial boundaries when numerical methods are applied. To make the truncated problem complete, special boundary conditions should be designed and applied at the artificial boundaries.

For truncating the unbounded domain, there are two main categories of methods which follow two different philosophies [Hagstrom, Bruno, et al. (2003); Antoine, Arnold, et al. (2008)]. The first one is using some exact boundary conditions, which are usually derived from the formal solutions or relations at the edges of the interested domain. The solution of the bounded problem coincides with the solution of the original unbounded problem in the interested domain. As a result, they are also referred as absorbing boundary conditions (ABCs) or transparent boundary conditions (TBCs) [Antoine, Besse, and Descombes (2006)]. The other method is using some absorbing layers to surround the interested domain, and the truncations are going to be done inside the additional layers. The equation is designed to be decaying in the layers, therefore the truncations will cause fewer reflections.

The most popular and mathematically elegant absorbing layer is called as the perfectly matched layer (PML), which was firstly introduced by Berenger for Maxwell's equations [Berenger (1994)]. Soon Chew and Weedom realized that the artificial boundary conditions using PMLs, or shortly the PML method, could be interpreted as a complex coordinate stretching inside the additional layers, in which the solution damps [Chew and Weedon (1994)]. In the following years, the PML method by complex coordinate stretching was generalized to more complicated settings and equations [Lu and Zhu (2007); Appelo, Hagstrom, and Kreiss (2007)]. This technique for bounding the computation domain has also been used for the Schrödinger equation [Hagstrom, Bruno, et al. (2003); Ahland, Schulz, and Voges (1999); Zheng (2007)].

In this paper, we focus on some problems when the PMLs are introduced to the computation of a kind of nonlinear Schrödinger (NSE) equations. In our computation, the time-splitting method is used to separate the nonlinearity, and the PMLs are added to limit the computation domain in solving the linear problems. A major feature of the PML is its absorbing function. In practice, the absorbing functions are varying sharply, therefore more grid points are needed to capture the profiles of the absorbing functions. Otherwise, the numerical errors would not be small as it is estimated in the error analysis [Nissen and Kreiss (2011)]. Since the absorbing functions in the interested domain are constants, we hope that the refinement could be done inside the PML only, in order to reduce the computation efforts and storage. In finite difference discretization, the direct refinement inside the PML will generate an uniform-but-unequal scheme, which is uniform separately inside and outside the PML but with two different step sizes. We have proved that this scheme will cause spurious reflections, even if the suitable interface conditions are

introduced. As a remedy, we have developed a new technique, which redistributes the grid points by an additional coordinate transformation, then the grid points are rearranged denser inside the PML. Since the refinement is done gradually, the unphysical reflection will not be observable.

The rest of this paper is organized as follows. In section 2, we explain the time-splitting scheme for the numerical simulation of nonlinear Schrödinger equations, and the PMLs are introduced in the spatial discretization of the linear problems. In section 3, we give a brief demonstration of the spurious reflections in the simulation of the linear Schrödinger equation with the uniform-but-unequal difference scheme, and also give a quantified analysis of the reflection ratio for simple cases. In section 4, the technique for redistributing grid points is introduced, which reduces the numerical reflections in long time computations. Examples and conclusions are presented in last two sections.

2 Time splitting method and PML

In this paper, a kind of semi-infinite Schrödinger equations are considered:

$$\begin{aligned} &i\partial_t u + \partial_x^2 u + \gamma|u|^{2\alpha}u = 0, x > 0, t > 0, \\ &u(0,t) = 0, \lim_{x\to+\infty} u(x,t) = 0, \\ &u(x,0) = u_0(x), \end{aligned} \tag{1}$$

where α is an integer and γ is a real constant. The nonlinearity contains a potential function dependent on $|u|^2$, which is common in practice. We assume that the initial function u_0 is mostly inside a finite region Ω_0. This assumption is essential for the efficiency of PML method.

2.1 The time splitting idea for NSE

In our computation, the time splitting method is used to separate the nonlinearity. That is to say, instead of solving the nonlinear problem (1), we turn to solve several linear problems and ODEs. During the computation, the discretization usually follows the method of lines, in other words, the spatial discretization is firstly introduced and the resulting system of ODEs can be solved by some suitable time-stepping methods.

Assume the temporal stepsize is τ, and $t_n = n\tau$, $U^n = u(x,t_n)$, the evolution from t_n to t_{n+1} is considered as follows. In order to separate the nonlinearity, we use Strang's second order splitting method [Strang (1968)], which achieves the accuracy of $O(\tau^2)$.

The first step is to solve an ODE:

$$i\frac{du}{dt}+\gamma|u|^{2\alpha}u=0 \tag{2}$$

in time sequence $[t_n,t_{n+1/2}]$, with the initial function given by U^n. When γ is real, we have

$$\frac{du}{dt}=i\gamma|u|^{2\alpha}u,\frac{d\bar{u}}{dt}=-i\gamma|u|^{2\alpha}\bar{u},$$

and

$$\frac{d}{dt}|u|^2=\frac{d}{dt}u\bar{u}=\bar{u}\frac{du}{dt}+u\frac{d\bar{u}}{dt}=0.$$

It is shown that $|u|^2$ is not time-dependent, therefore (2) can be replaced by

$$i\frac{du}{dt}+\gamma|U^n|^{2\alpha}u=0, \tag{3}$$

which is analytically solvable over $[t_n,t_{n+1/2}]$, and the solution is:

$$u=U^n e^{i(t-t_n)\gamma|U^n|^{2\alpha}}.$$

Let

$$U^*=u|_{t=t_{n+1/2}}=U^n e^{\frac{i\tau}{2}\gamma|U^n|^{2\alpha}}.$$

The second step is to solve a linear Schrödinger (LS) equation

$$i\partial_t u+\partial_x^2 u=0,x>0,t_n<t<t_{n+1} \tag{4}$$

with the initial function given by U^*.

To solve the semi-infinite linear problem, different methods based on different spatial discretization and boundary conditions could be used. The methods based on finite element are well-defined and widely used [Han and Huang (2004)], nevertheless they are less extended and the implementations are difficult in practice. The spectral methods [Bao, Jin, and Markowich (2002)], or pseudo-spectral methods, are global approximations which achieve high accuracy with relatively few grid points. However, there are few literatures using the spectral method in domains with PMLs. This is mainly reason that accuracy of pseudo-spectral method depends on smoothness of the functions, which is poor in the PML cases. In the same time, finite differences are flexible in terms of boundary conditions and spatial adaptivity, and easy to implement in practical computations. In this paper, PML

method is applied to truncate the domain, and the finite difference method is used in the discretization of the LS equation with PML.

The third step is to solve (2) again in time sequence $[t_{n+1/2}, t_{n+1}]$ to complete the evolution, with the initial function given by the solution of equation (4) at $t = t_{n+1}$, namely U^{**}, where $|u|^2$ is replaced by $|U^{**}|^2$. In the same manner, we obtain

$$U^{n+1} = U^{**} e^{\frac{i\tau}{2}\gamma|U^{**}|^{2\alpha}}.$$

2.2 PML with coordinate stretching

The PML method is involved in the second step. A most important property of the PML is that wave can penetrate the interface between the interested physical domain and the PML without any reflection. Moreover, the wave inside the PML decays exponentially along the propagating axis, therefore the direct truncation in a short distance inside the absorbing layer will not induce many reflections. Mathematically, it equals that a coordinate stretching is applied inside the PML region, which makes the wave damped. Using the definition of coordinate stretching, PML is easy to extend to the unbounded linear Schrödinger equation

$$i\partial_t u + \partial_x^2 u = V(x)u,\ x > 0. \tag{5}$$

For a general discussion, we consider the linear case when the potential function is $V = V(x)$, which is assumed to be constant outside a finite region Ω'. We focus on the solution inside $\Omega = \Omega_0 \bigcup \Omega'$. It is also called as the interested physical domain. In the 1D case, it can be set as $[0, H]$. Considering the exterior problem when $x > H$, we have $V(x) = V_r$ and

$$i\partial_t u + \partial_x^2 u = V_r u,\ x > H. \tag{6}$$

Let the modal solution be $u = e^{\lambda x + st}$, where s with $\mathrm{Re}(s) > 0$ is the argument in the Laplace-transformed space. Substituting into (6), it turns out $is + \lambda^2 = V_r$. Since the solution vanishes when the wave travels toward infinity, we have

$$\lambda = -\sqrt{-is + V_r},$$

in which the square root is chosen to satisfy $\mathrm{Re}(\sqrt{-is + V_r}) > 0$. It is easy to verify that λ is in the second quadrant. The PML is added in the exterior region $\{x > H\}$, in which the transformation

$$\bar{x} = x + R\int_H^x \sigma(r)dr \tag{7}$$

is applied. In (7), R is a complex number, and the real function σ is referred as the absorbing function, which is a very important feature of PML. With the transformation (7), the modal solution inside the PML is therefore

$$\bar{u} = e^{\lambda \bar{x}+st} = e^{\lambda x+st} e^{\lambda R \int_H^x \sigma(r)dr}.$$

To make the solution damped, the real part of λR must be negative. As mentioned above, λ is in the second quadrant. So the complex number $R = e^{i\theta}$ can take values with θ between 0 and $\pi/2$. In this paper, $R = e^{i\pi/4}$ is used for average. Notice that

$$\frac{\partial \bar{x}}{\partial x} = 1 + R\sigma(x),$$

the damped solution $\bar{u}$ satisfies

$$i\partial_t \bar{u} + c\partial_x(c\partial_x \bar{u}) = V_r \bar{u},$$

with $c = 1/(1+R\sigma)$ for $x \in (H, +\infty)$, while it satisfies the original equation (5) in Ω.

Waves inside the PML decay exponentially, therefore the direct truncation at $H+d$ for some $d > 0$ will not introduce notable reflections, the solution inside Ω is thus almost the same as that of original problem (5).

If the thickness of PML is d, (5) is approximated by the bounded problem:

$$\begin{aligned} &i\partial_t u + c\partial_x(c\partial_x u) = V(x)u, \quad x \in [0, H+d], \\ &u(0,t) = u(H+d,t) = 0, \end{aligned} \tag{8}$$

where $\sigma(x) = 0$ inside the interval $[0,H]$. The relation $\sigma(H) = 0$ and $\sigma'(H) = 0$ must be satisfied to keep the non-reflection property. Though it is not a sufficient condition.

3 the spurious reflection on nonuniform grid

The PML-modified equation has the coefficient $c(x)$, which depends on the absorbing function $\sigma(x)$. Usually σ varies very fast. And the reflections of PML method mostly come from the numerical discretization of the PML profile. Based on these facts, more points are needed inside the PML to make the numerical reflections small. In order not to increase too much computation efforts and storage, and making use of the property that $\sigma(x) = 0$ inside the interested region Ω, we hope that grid points only inside the PML could be refined uniformly. Unfortunately, this kind of finite difference scheme would approximate the dispersion relation differently on both side of the interface, and therefore induce spurious reflections. The

reflections do not physically exist and are not avoidable in this uniform-but-unequal scheme even when some suitable interface conditions are added. Whether the PML exists or not, this kind of discretization is not available due to the unphysical reflections. Similar to Vichnevetsky (1981) for wave equations, the remaining of this section will demonstrate this fact and quantify the spurious reflections for some simple cases. A remedy will be introduced in next section.

For convenience, we take no account of the PML, and consider the linear homogenous Schrödinger equation $i\partial_t u + \partial_{xx} u = 0$ for the discussion of spurious reflections. In the continuous version, the dispersion relation is

$$\omega = -\kappa^2, \tag{9}$$

when the planewave solution $e^{i(\kappa x - \omega t)}$ is inserted into the equation. Using the uniform finite difference scheme in space, we have

$$i\partial_t u_j + \frac{u_{j-1} - 2u_j + u_{j+1}}{h^2} = 0, \tag{10}$$

at the point x_j. Insert the semi-discrete planewave solution $u_j(t) = e^{i(\kappa jh - \omega t)}$, the dispersion relation for the semi-discrete equation is

$$\omega = -\frac{4\sin^2(\kappa h/2)}{h^2}. \tag{11}$$

It converges to (9) when h tends to zero.

Applying the Fourier transformation with respect to time in (10), it turns to

$$-\omega \hat{u}_j + \frac{\hat{u}_{j-1} - 2\hat{u}_j + \hat{u}_{j+1}}{h^2} = 0.$$

It has an equivalent matrix form:

$$\hat{U}_j = S\hat{U}_{j-1}, \tag{12}$$

where

$$\hat{U}_j = \begin{bmatrix} \hat{u}_{j+1} \\ \hat{u}_j \end{bmatrix}, S = \begin{bmatrix} 2z & -1 \\ 1 & 0 \end{bmatrix},$$

and $z = 1 + \omega h^2/2$. The matrix S depends on ω and h, and it can be diagonalized as $S = XDX^{-1}$, where

$$X = \begin{bmatrix} r & l \\ 1 & 1 \end{bmatrix}, D = \begin{bmatrix} r & 0 \\ 0 & l \end{bmatrix},$$

with $r = z + \sqrt{z^2-1}, l = z - \sqrt{z^2-1}$. So

$$\hat{U}_j = XDX^{-1}\hat{U}_{j-1}. \tag{13}$$

Denote that $\hat{C}_j = X^{-1}\hat{U}_j$, (13) can be rewritten as

$$\hat{C}_j = D\hat{C}_{j-1}. \tag{14}$$

In fact,

$$\hat{U}_j = \begin{bmatrix} \hat{u}_{j+1} \\ \hat{u}_j \end{bmatrix} = X\hat{C}_j = \begin{bmatrix} r & l \\ 1 & 1 \end{bmatrix} \begin{bmatrix} \hat{c}_{r,j} \\ \hat{c}_{l,j} \end{bmatrix},$$

where the vector $\hat{C}_j = \begin{bmatrix} \hat{c}_{r,j} & \hat{c}_{l,j} \end{bmatrix}^T$ is the decomposition of the wave along the propagating axis, i.e. $\hat{u}_j = \hat{c}_{r,j} + \hat{c}_{l,j}$. And the diagonal matrix D characterizes the behaviors of wave during the spatial shifting. As mentioned above,

$$D = \begin{bmatrix} z + \sqrt{z^2-1} & 0 \\ 0 & z - \sqrt{z^2-1} \end{bmatrix},$$

with $z = 1 + \omega h^2/2$ and $\omega = -4\sin^2(\frac{\kappa h}{2})/h^2$, the value of r and l are either real or complex. As a result, the wave has either the propagation or the diffusion behavior with different frequency, which is consistent with the solution of LS equation.

When the discretization is uniform, the decomposition of S is identical in every sequence, X is cancelled in each spatial transition. Therefore,

$$\hat{C}_N = D^N\hat{C}_0,$$

the dispersion relation is approximated correctly.

However, by the nonuniform discretization, the situation is much more different. Suppose that the computation grids are divided into two parts: the step size of the first part at the left hand side is h_1, while that of the second part is h_2. We impose the interface conditions carefully as follows. If the interface point is x_d, we set the continuous conditions as:

$$u(x_d-) = u(x_d+), \frac{du(x_d-)}{dx} = \frac{du(x_d+)}{dx}.$$

To approximate these conditions, we set the grid points $x_N = x_d - h_1/2$, $x_{N+1} = x_d + h_2/2$. In this case, the interface x_d is not a grid point, but half step sizes to the nearest grid points each side. Using the symmetric extension points, we can present the second order derivative together with the continuous conditions. It is to say, we set $x'_{N+1} = x_d + h_1/2, x'_N = x_d - h_2/2$ as the symmetric points of x_N and x_{N+1}

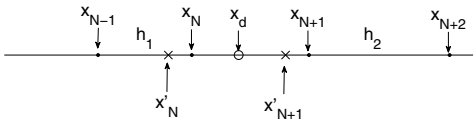

Figure 1: The 'uniform-but-unequal' discretization, both left and right of the point x_d are discretized uniformly, but the step sizes of both sides are different.

with respect to x_d, and denote $\hat{u}'_{N+1} = \hat{u}(x'_{N+1}), \hat{u}'_N = \hat{u}(x'_N)$. This is shown in Fig.1. With this treatment on the interface, the second derivative of u at x_N, x_{N+1} could be expressed as:

$$\partial_x^2 u_N \approx \frac{\hat{u}_{N-1} - 2\hat{u}_N + \hat{u}'_{N+1}}{h_1^2},$$
$$\partial_x^2 u_{N+1} \approx \frac{\hat{u}'_N - 2\hat{u}_{N+1} + \hat{u}_{N+2}}{h_2^2}.$$

And the interface conditions are approximated as:

$$\begin{aligned} \frac{\hat{u}_N + \hat{u}'_{N+1}}{2} &= \frac{\hat{u}'_N + \hat{u}_{N+1}}{2}, \\ \frac{\hat{u}'_{N+1} - \hat{u}_N}{h_1} &= \frac{\hat{u}_{N+1} - \hat{u}'_N}{h_2}. \end{aligned} \tag{15}$$

For each uniform discrete part of the computation domain, the spatial transmission relation is similar to (13), except that the matrix X is not always the same.

$$\begin{bmatrix} \hat{u}_{N+2} \\ \hat{u}_{N+1} \end{bmatrix} = X_{N+1} D_{N+1} X_{N+1}^{-1} \begin{bmatrix} \hat{u}_{N+1} \\ \hat{u}'_N \end{bmatrix},$$

$$\begin{bmatrix} \hat{u}'_{N+1} \\ \hat{u}_N \end{bmatrix} = X_N D_N X_N^{-1} \begin{bmatrix} \hat{u}_N \\ \hat{u}_{N-1} \end{bmatrix}.$$

Due to the interface conditions (15), we have the relation

$$\begin{bmatrix} \hat{u}_{N+1} \\ \hat{u}'_N \end{bmatrix} = H \begin{bmatrix} \hat{u}'_{N+1} \\ \hat{u}_N \end{bmatrix},$$

where

$$H = \begin{bmatrix} 1 & 1 \\ \frac{1}{h_2} & -\frac{1}{h_2} \end{bmatrix}^{-1} \begin{bmatrix} 1 & 1 \\ \frac{1}{h_1} & -\frac{1}{h_1} \end{bmatrix}.$$

The transmission relation across the interface is therefore

$$\hat{U}_{N+1} = X_{N+1} D_{N+1} X_{N+1}^{-1} H X_N D_N X_N^{-1} \hat{U}_{N-1}. \tag{16}$$

Similarly, since $X_{N+2} = X_{N+1}$, we have

$$\hat{C}_{N+1} = D_{N+1} X_{N+1}^{-1} H X_N D_N \hat{C}_{N-1}. \tag{17}$$

Obviously, $X_{N+1}^{-1} H X_N \neq I$ with our H, thus the dispersion relation is not correctly approximated. The reflections will therefore occur due to the difference between X_N and X_{N+1}. They do not physically exist, but disturb the computation badly.

If we assume there is a right-moving wave in $\{x < x_d\}$ and no left-moving wave in $\{x \geq x_d\}$, we can solve for the reflection ratio $\rho = |\hat{c}_{l,N}/\hat{c}_{r,N}|$ by inserting $\hat{c}_{l,N+1} = 0$ to (17), to give

$$\rho = \frac{r_N}{l_N} \frac{(1-h_1/h_2)(r_N r_{N+1} - 1) + (1+h_1/h_2)(r_{N+1} - r_N)}{(1-h_1/h_2)(l_N r_{N+1} - 1) + (1+h_1/h_2)(r_{N+1} - l_N)}$$

The reflection ratio grows when the difference between h_1 and h_1 becomes larger. And it vanishes in the case $h_1 = h_2$, where $r_N = r_{N+1}$.

4 the redistributing technique for the discretization of PML

Because of the spurious reflections, we cannot capture the profile of absorbing function more efficiently by using finer grids only inside PML. Considering that the reflections appear as soon as the spatial step size changes abruptly, we are proposing another nonuniform discrete scheme by reducing the step size gradually, which results in relatively more grid points in the PML region. And the numerical reflections due to PML are smaller comparing to the uniform-but-unequal case. This improvement is useful when concerning the wave that is impacting with PML.

To do this, we introduce a coordinate transformation which increases the density of grid points in the PML region. For example, if we are considering the linear homogenous Schrödinger equation on $[0,H]$, and a PML of thickness d is added on the right hand side; and suppose the absorbing function of the PML is $\sigma(x)$, and therefore $c(x) = \frac{1}{1+R\sigma(x)}$. Then the modified equation with a PML is

$$i\partial_t u + c(x)\partial_x c(x)\partial_x u = 0, x \in [0, H+d], \tag{18}$$

where $c(x) = 1$ for $x \in [0,H]$. Our goal is to move some grid points into the PML region $[H, H+d]$ with the help of the coordinate transformation. Consider the function

$$x = \frac{\tanh(r_0 \xi/(H+d))}{\tanh r_0}(H+d), \tag{19}$$

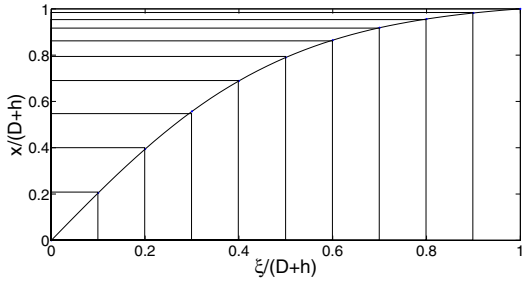

Figure 2: The function $\tanh(r_0\xi)/\tanh r_0$ with $r_0 = 2$. It maps the uniform grid on ξ-plane to non-uniform grid on x-plane, which is denser for large x.

where r_0 is a given parameter, it is easy to see that it maps the uniform grid points on ξ to the nonuniform ones on x, as plotted in Fig.2, which just meets our demand. However, in the numerical computation, the discrete points are distributed uniformly over $[0, H+d]$ on ξ-plane. And look into the x-plane, more points are therefore inside the PML region.

To solve the equation (18), it is transformed to the ξ-plane. We have

$$\frac{dx}{d\xi} = \frac{r_0}{\tanh r_0 \cosh^2(r_0\xi/(H+d))},$$

the Schrödinger equation on ξ-plane is:

$$i\partial_t u + p(\xi)\partial_\xi p(\xi)\partial_\xi u = 0, \xi \in [0, H+d], \tag{20}$$

where $p(\xi) = \frac{\tanh r_0}{r_0} c(x(\xi)) \cosh^2(r_0\xi/(H+d))$. An additional coordinate transformation (19) other than the PML-transformation (7) is introduced to redistribute the grid points. The procedure for solving Eq. (20) is the same as (18) except that $c(x)$ is replaced by $p(\xi)$.

The method for nonlinear equations (1) is similar, when the PML is involved in the second step with solving the linear problems. The numerical examples in the next section will show this fact.

5 numerical results

To show the impact of our method, we compute the semi-infinite linear problem (18) in the previous section. We set $H = 5$, and the thickness of PML is $d = 1$. The absorbing function is

$$\sigma(x) = \frac{\sigma_0 \tau(x)^5}{1+\tau(x)^2}, \tag{21}$$

where $\tau(x) = \max(x-H, 0)$, and σ_0 is the absorbing strength factor. It is a generalization of polynomial absorbing functions in Nissen and Kreiss (2011), and it varies more sharply. We use $\sigma_0 = 100$ here. The initial function is

$$u_0(x) = e^{-(x-2.5)^2 + ik_0(x-2.5)},$$

and thus the exact solution is

$$u_e(x,t) = \sqrt{\frac{i}{-4t+i}} \exp \frac{-i(x-2.5)^2 - k_0(x-2.5) + k_0^2 t}{-4t+i}.$$

We use the method of lines, in which the spatial discretization is firstly introduced, for example $c\partial_x c\partial_x u \approx D_2$ or $p\partial_x p\partial_x u \approx \tilde{D}_2$. The uniform discrete scheme and the coordinate-transformed scheme are both used in different computations. We keep $\Delta x = \Delta\xi = 0.02$ for comparison. And the Crank-Nicolson scheme is used afterwards for time evolution as

$$\frac{U^{n+1} - U^n}{\tau} = \frac{i}{2} D_2 (U^{n+1} + U^n).$$

The C-N scheme is unconditionally stable in time, we use the temporal step size $\tau = 0.0005$ here, and the result is plotted in Fig.3, where the phase velocity of the initial wave is $k_0 = 2$. A comparison of relative errors is also plotted in Fig.4, where the relative error is defined by:

$$\varepsilon(t_n) = \frac{\| U^n - u_e(x,t_n) \|_{[0,H]}}{\| u_e(x,t_n) \|_{[0,H]}}$$

which concerns only the solutions inside the interested domain $[0,H]$ with L^2-norm. It can be seen in Fig.3 that the uniform discrete PML works very well, since it absorbs the incoming waves as soon as it enters the PML at $x = H$. The reflections are too small to be observed. However, by comparing the relative errors, we know that the uniform discrete scheme works better at the first stage, in which the wave does not reach the PML, and the discretization error of the interested domain dominate. Later on, as the PML continuously comes into work, the error from the discretization of PML plays a more and more important role. As the figure shown, after about $t > 0.5$, the coordinate-transformed scheme with parameter $r_0 = 4$ works better and better, since it captures the profile of absorbing function better, and therefore reduces the discretization error from PML.

To show the invalidity of the uniform-but-unequal scheme as in Section 3, we compute the same case with this scheme. In order to make the numerical reflections at the interface more observable, PMLs are added to remove the reflections at the

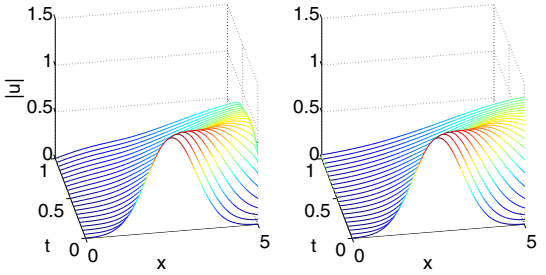

Figure 3: The solution of linear equation $i\partial_t u + \partial_{xx} u = 0$. Left: numerical solution with PML which is uniformly discrete. Right: the exact solution.

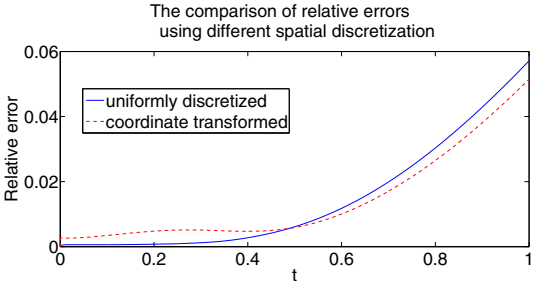

Figure 4: The comparison of relative errors using different spatial discretization.

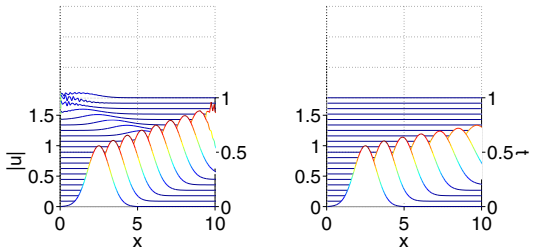

Figure 5: The spurious reflection due to the different step sizes in different part of the domain. Left: the solution with uniform-but-unequal scheme. Right: the solution with uniform scheme.

boundary. An initial wave with phase velocity $k_0 = 10$ is used. The spatial step in the interested domain is $h_1 = 0.1$, while that in the PML is $h_2 = 0.02$. The spurious reflection is easy to be observed in the left plot of Fig.5, therefore the result is not trustable.

Finally, return to our major topic: the nonlinear Schrödinger equations (1). Considering an instance of (1) with $\gamma = 2, \alpha = 1$. That is

$$i\partial_t u + \partial_x^2 u + 2|u|^2 u = 0,$$

which supports the exact solution

$$u_e(x,t) = \sqrt{a} * \operatorname{sech}\sqrt{a}(x-3-ct)e^{i(\frac{c}{2}(x-3)+(a-\frac{c^2}{4})t)},$$

the interested domain is $[0,10]$ with a PML with the thickness $d = 1$, whose profile is the same as (21). The time-splitting scheme which introduced in section II is used. The transformation (19) with $r_0 = 2$ is used in the spatial discretization. We use $a = 2$, $c = 15$ here as in Zheng (2007), and the remaining parameters are $t_{max} = 0.8$, $\tau = 0.0005$, $h = 0.02$. The picture is shown in Fig.6, for nonlinear Schrödinger equation, our method works as well.

6 conclusions

The PML is widely used in the simulation of problems on unbounded domain, it is flexible and easy to implement in practice. However, in the computation of time dependent problems, we have observed the phenomena that the PML becomes less efficient as time goes by. One of the possible reasons is that the error from the discretization of PML increases when the wave goes deep into the layer. This error mostly comes from the discretization of the corresponding absorbing function, which varies sharply in most of the cases. In order to improve the performance of PML, we have considered several non-uniform finite difference scheme in this paper. Firstly, we have proved that the uniform-but-unequal scheme is not feasible due to the spurious reflection. It is proved that the temptation of directly refinement inside the PML region is invalid. Next, we propose a new method which uses an additional coordinate transformation to redistribute the grid points, in order to make it denser in PML. We move more points into the PML region, then the profile of absorbing function is better captured, and the discretization error turns smaller. This method is more accurate, especially when the PML begins to absorb the waves. Numerical results have shown that it works better than the uniform PML in long time computation of TDSE.

Acknowledgments

This work was partially supported by the Natural Science Foundation of China under the Grant (No.11071217), and the Natural Science Foundation of Zhejiang Province,China under the Grant (No.Y6100210).

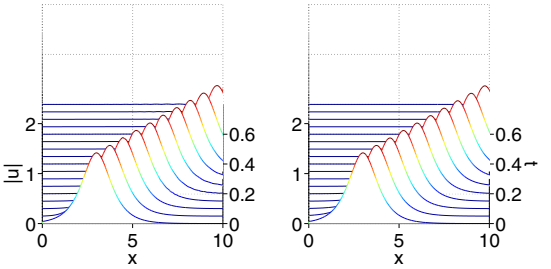

Figure 6: Solution of nonlinear Schrödinger equation using our method. Left: the solution using our coordinate transformation. Right: the exact solution.

References

Ahland, A.; Schulz, D.; Voges, E. (1999): Accurate mesh truncation for Schrödinger equations by a perfectly matched layer absorber: Application to the calculation of optical spectra. *Physical Review B*, vol. 60, no. 8, pp. 5109–5112.

Antoine, X.; Arnold, A. et al. (2008): A review of transparent and artificial boundary conditions techniques for linear and nonlinear Schrödinger equations. *Commun. Comput. Phys.*, vol. 4, no. 4, pp. 729–796.

Antoine, X.; Besse, C.; Descombes, S. (2006): Artificial Boundary Conditions for One-Dimensional Cubic Nonlinear Schrodinger Equations. *SIAM Journal on Numerical Analysis*, vol. 43, no. 6, pp. 2272–2293.

Appelo, D.; Hagstrom, T.; Kreiss, G. (2007): Perfectly matched layers for hyperbolic systems: general formulation, well-posedness, and stability. *SIAM Journal on Applied Mathematics*, vol. 67, no. 1, pp. 1–23.

Bao, W.; Jin, S.; Markowich, P. (2002): On time-splitting spectral approximations for the Schrödinger equation in the semiclassical regime. *Journal of Computational Physics*, vol. 175, no. 2, pp. 487–524.

Berenger, J. (1994): A perfectly matched layer for the absorption of electromagnetic waves. *Journal of computational physics*, vol. 114, no. 2, pp. 185–200.

Chew, W.; Weedon, W. (1994): A 3D perfectly matched medium from modified Maxwell's equations with stretched coordinates. *Microwave and optical technology letters*, vol. 7, no. 13, pp. 599–604.

Hagstrom, T.; Bruno, O. et al. (2003): New results on absorbing layers and radiation boundary conditions. *Topics in Computational Wave Propagation-Direct and Inverse Problems*, vol. 1, pp. 42.

Han, H.; Huang, Z. (2004): Exact artificial boundary conditions for Schrödinger equation in R2. *Comm. Math. Sci*, vol. 2, no. 1, pp. 79–94.

Lu, Y.; Zhu, J. (2007): Perfectly matched layer for acoustic waveguide modeling-Benchmark calculations and perturbation analysis. *CMES: Computer Modeling in Engineering and Sciences*, vol. 22, no. 3, pp. 235.

Nissen, A.; Kreiss, G. (2011): An optimized perfectly matched layer for the Schrödinger equation. *Commun. Comput. Phys.*, vol. 9, no. 1, pp. 147–179.

Strang, G. (1968): On the construction and comparison of difference schemes. *SIAM Journal on Numerical Analysis*, vol. 5, no. 3, pp. 506–517.

Vichnevetsky, R. (1981): Propagation Through Numerical Mesh Refinement for Hyperbolic Equations. *Math. & Comp. in Simul.*, vol. 23, no. 4, pp. 344–353.

Zheng, C. (2007): A perfectly matched layer approach to the nonlinear Schrödinger wave equations. *Journal of Computational Physics*, vol. 227, no. 1, pp. 537–556.